Analyst

PAPER

View Article Online
View Journal

Cite this: DOI: 10.1039/c6an00694a

Label-free, ITO-based immunosensor for the detection of a cancer biomarker: Receptor for Activated C Kinase 1†

E. B. Bahadır[a] and M. K. Sezgintürk*[b]

A new, quite sensitive disposable immunosensor, based on the anti-RACK1 antibody, was developed for the determination of Receptor for Activated C Kinase 1 (RACK1) for the first time. Moreover, indium tin oxide (ITO) flexible sheets were modified by using aldehyde ended silane 11-(triethoxysilyl)undecanal (TESU) self-assembled monolayers (SAMs) for immobilizing the anti-RACK1 antibody *via* covalent bonds. Cyclic voltammetry (CV), electrochemical impedance spectroscopy (EIS), and square wave voltammetry (SWV) methods were used for characterizing the immobilization steps and for determining the RACK1 concentration. To obtain a successful immunosensor, experimental factors were optimized. This quite sensitive biosensor was able to detect concentrations as low as fg mL^{-1}. The detection principle was based on the change in charge transfer resistance and the Nyquist plot diameter and these changes were monitored by using electrochemical impedance spectroscopy (EIS). This impedimetric immunosensor had perfect repeatability and reproducibility. We proved that the new silane agent, TESU, performs well in biosensor applications. The feasibility of the fabricated immunosensor was tested by detecting RACK1 in artificial and real human serum samples.

Received 23rd March 2016,
Accepted 13th July 2016

DOI: 10.1039/c6an00694a

www.rsc.org/analyst

Introduction

The Receptor for Activated C Kinase 1 (RACK1) is a protein which belongs to the tryptophan-aspartate repeat (WD-repeat) family[1] and a homologue of the β-subunit of G-protein.[2,3] RACK1 is a 36 kDa adaptor protein and has 7 WD40 repeats.[3,4] The WD40 repeats of RACK1 are responsible for complex protein–protein interactions between signalling molecules such as phosphodiesterase 4D5, β-integrins, and Src tyrosine kinase, as well as protein kinase C (PKC) 1, which are responsible for cell growth, movement, and division.[5] Also, RACK1 can be an effective cancer biomarker for some tumour types, such as oral squamous cell carcinoma,[5,6] melanoma,[5] colon cancer,[2,5] non-small cell lung cancer,[2,5] hepatocellular carcinoma[5] and breast cancer.[1,7] In breast cancer, RACK1 is known as an independent prognostic factor and it supports proliferation and metastasis *in vitro*/*vivo*. Sensitive and accurate determination of cancer biomarkers, which are used in diagnostic tests, has become an important issue recently. In particular, the monitoring of cancer biomarkers in serum has a significant role for early cancer diagnosis.[8]

EIS is a tool, which is utilized for monitoring the structure and function of a variety of biosensors such as immunosensors, DNA biosensors and enzyme based biosensors. Impedimetric immunosensors have gained importance because they enable direct and label-free detection of biomolecules. In an EIS technique, immunodetection of a biomolecule is associated with the differences between the electron transfer resistances. Also, this change depends on the amount of antibodies immobilized on the electrode surface and the interaction between the antibody and its antigen. After interaction between the antigen and the antibody, which is immobilized on the electrode surface, a remarkable difference is observed in the electron transfer resistance due to this interaction.

Self-assembled monolayers (SAMs) have been utilized for fabrication of ITO electrodes. The self-assembled monolayers can be monitored using electrochemical techniques, and they also provide selective electrodes for electroanalytical applications. For the construction of stable and well-structured alkyl silane monolayers on ITO thin films, a pre-treatment process is required. For modifying of SAMs on the ITO electrodes, many surface attachment methods have been described in the literature.[9–11] Silanization of ITO based substrates are the most preferred methods for modifying of ITO electrodes. The end group of SAMs is made up of chemically bound biorecognition elements. A key aspect of the fabrication of a

[a]*Namık Kemal University, Scientific and Technological Research Center, Tekirdağ, Turkey*
[b]*Namık Kemal University, Faculty of Science, Chemistry Department, Biochemistry Division, Tekirdağ, Turkey. E-mail: msezginturk@hotmail.com, msezgintürk@nku.edu.tr; Tel: +90 282 250 2605*

†Electronic supplementary information (ESI) available. See DOI: 10.1039/c6an00694a

biosensor is the immobilization of biorecognition elements such as antibodies, receptors, enzymes or DNA on the electrode surface. The choice of biorecognition element affects the selectivity of biosensors, considerably.[9] In the literature ITO based substrates were employed as the working electrode for pathogenic bacteria,[10–12] cancer biomarkers,[13–16] estradiol,[17] H_2O_2,[18–20] glucose,[21] cholesterol,[22] tryptophan[23] and immunoglobulin G.[24] Many of these studies mentioned above applied the same procedure; ITO thin films were firstly cleaned and pre-treated to introduce hydroxyl groups on the surface of the ITO covering. Then ITO electrodes were modified with silane molecules such as (3-isocyanatopropyl) triethoxysilane (IPTES),[9] 3-aminopropyltriethoxy silane (APTES),[13,16,19,23] (3-glycidoxypropyl) trimethoxysilane,[11] *N*-(2-aminoethyl)-3-amino propyltrimethoxysilane,[25] 3-mercaptopropyl trimethoxysilane (3-MPTMS),[18] 3-glycidoxy propyldimethoxysilane.[10] Apart from this procedure, electrodeposition of nanoparticles on the ITO thin film was also used in several studies.[21,25,26]

In the diagnosis and treatment of cancer, rapid and sensitive detection of biomarkers has a vital role. In this study, we fabricated an impedimetric biosensor based on ITO thin films covered on a flexible polyethylene terephthalate substrate for the detection of a cancer biomarker, RACK1. The ITO based substrate was chosen as a working electrode owing to its perfect optical transparency, high electrical conductivity, wide electrochemical working window and stable electrochemical and physical features.[13–15] All these features supported the usability of ITO thin films to develop a biosensor for the detection of various biomolecules. In this study, an ITO electrode was firstly cleaned and activated and after activation of the surface, it was modified with 11-(triethoxysilyl)undecanal (TESU) to form a highly structured SAM. Subsequently, anti-RACK1 antibodies were immobilized on the SAMs without using any crosslinker. CV and EIS are very important tools for monitoring interface information between the electrode and the electrolyte solution. In this study, biorecognition events on the electrode surface were monitored by EIS and CV, and a strong interaction was found between the anti-RACK1 antibody and its ligand RACK1. Moreover, the SWV technique was also performed to plot the RACK1 calibration curve. Apart from these electrochemical techniques, scanning electron microscopy (SEM) images were obtained to identify the morphological appearance of the different layers obtained during the immobilization steps. The fabrication parameters of the novel immunosensor such as anti-RACK1 concentration, anti-RACK1 binding period, RACK1 concentration and RACK1 binding period were also optimized.

Materials and methods

Reagents and materials

High-purity chemicals were purchased from Sigma-Aldrich (St Louis, MO, USA). ITO-coated PET films, which have a surface resistivity of 60 Ω^2 and transmittance at 550 nm (>79%), and biorecognition elements (anti-RACK1 antibody and RACK1) were obtained from Sigma-Aldrich (St Louis, MO, USA). Anti-RACK1 antibody, RACK1 and bovine serum albumin (BSA, 0.5%) were prepared by using a phosphate buffer (50 mM, pH 7.0) and were kept at −20 °C. A redox probe solution, which contains 1 M KCl, 5 mM $[Fe(CN)_6]^{4-}$ and 5 mM $[Fe(CN)_6]^{3-}$ in phosphate buffer (50 mM, pH 7.0) was prepared. Artificial serum samples were prepared by using 4.5 mM KCl, 1.6 mM $MgCl_2$, 2.5 mM urea, 145 mM NaCl, 5 mM $CaCl_2$, 4.7 mM D-glucose and 0.1% human serum albumin.

Apparatus

Electrochemical measurements were carried out *via* a Gamry Potentiostat/Galvanostat (Reference 600, Gamry Instruments, Warminster, PA, USA) connected with a computer *via* EChem Analyst software. A three electrode system which was comprised of a sheet of ITO thin film (2 × 20 mm) as a working electrode, a platinum wire as a counter electrode and a silver/silver chloride as a reference electrode. The reference electrode and counter electrode were purchased from BASi (West Lafayette, IN, USA).

Preparation of electrodes before modification

ITO electrodes were cleaned by ultrasonication for 10 min with acetone, soap solution, followed by ultra-pure water. After drying with a stream of high purity argon, electrodes were immersed in a mixed solution of ultra-pure water/hydrogen peroxide/ammonium hydroxide (5 : 1 : 1, v/v) for 90 min to obtain the hydroxylated active ITO surface in dark conditions. Then activated ITO surfaces were washed with ultra-pure water and dried by using argon gas.

Stepwise modification of ITO electrodes

The activated ITO electrodes were immersed into the 0.25% 11-(triethoxysilane)undecanal (TESU) solution prepared in ethanol overnight. Thus, aldehyde groups were introduced onto ITO electrode surfaces. Then they were washed with ultra-pure water and dried with Argon stream. Subsequently, aldehyde modified ITO based substrates were immersed into anti-RACK1 antibodies (0.1625 ng mL^{-1} solution in PBS) for 1 h at room conditions and were washed with ultra-pure water to eliminate physically linked anti-RACK1 antibodies. In the last step, the modified ITO electrodes dipped in BSA solution (0.5%) at room temperature to avoid non-specific bindings. The immunosensor fabrication procedure is illustrated in Scheme 1.

Experimental measurements

For characterization of the modification and immobilization steps of the ITO electrode, CV, EIS and SWV were utilized. These electrochemical measurements (CV, EIS, and SWV) were performed in a 5 mM $K_3[Fe(CN)_6]/K_4[Fe(CN)_6]$ (1 : 1) solution that contains 0.1 M KCl. Unless indicated otherwise, CV (scan rate:100 mv s^{-1}, step size:10 mV), EIS (initial frequency: 50 000 Hz, final frequency: 0.05 Hz, points: 5), and SWV (potential scan range: 0–1.2 V, pulse size: 25 mV) measurements were carried out by using the same electrochemical parameters.

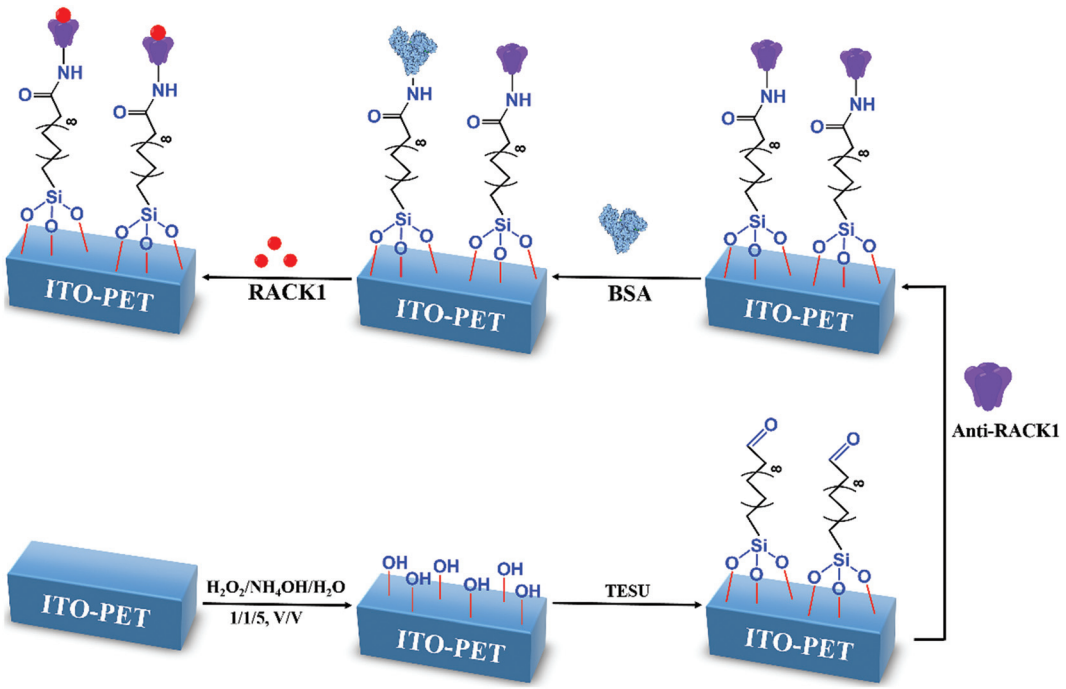

Scheme 1 Schematic illustration of the immunosensor.

SEM studies

The surface morphology of electrodes was elucidated through monitoring by a field emission scanning electron microscope (FEI-Quanta FEG 250 model). The SEM measurement was performed at the Scientific and Technological Research Center of Namık Kemal University (NABİLTEM). To obtain the SEM images 5 kV was used as an acceleration voltage.

Results and discussion

Immobilization of the anti-RACK1 antibody onto the ITO electrode

The whole procedure followed for the fabrication of the immunosensor is demonstrated in Scheme 1. The first step for fabrication of an immunoelectrode was cleaning of the ITO electrode surface. This step was important because possible organic contaminants on the ITO surface could affect the response of the electrode. After that, the ITO surface was activated by forming hydroxyl groups as mentioned previously. The hydroxylated ITO was exposed to TESU. Thus, silane SAMs containing active aldehyde groups, which were reactive to the anti-RACK1 antibody, were formed on the electrode surface spontaneously.[27] TESU enabled the straightforward covalent immobilization of the biorecognition elements without the need of using crosslinking agents.[28] Antibodies can be immobilized on the ITO surface through chemical covalent bonding with the reaction between the aldehyde group and the amino group of an antibody.[29] Then the ITO surface was blocked by a BSA solution to avoid non-specific binding. In this way, an impedimetric immunosensor was successfully constructed for RACK1 detection, for the first time as reported in this research.

In this study, fabrication of the immunosensor was monitored by CV and EIS. The $K_3[Fe(CN)_6]/K_4[Fe(CN)_6]$ couple was a convenient tool for analysing the electron transfer between the electrolyte solution and the electrode surface and it was used as a redox couple for many different electrochemical processes. The insulating features of any given ITO surface can be easily monitored by using this redox couple. Thereby, information about the adsorbed layers can be obtained.

EIS is an electrochemical technique, which enables the investigation of the modification steps of an electrode *via* changes in interface features. EIS has been employed for monitoring the interface information and biorecognition events. This significant tool provided information about the electrode fabrication and optimization steps. The impedance spectra of each immobilization step of the immunosensor are illustrated in Fig. 1A. It represents a Nyquist plot for modified ITO surfaces. $Fe(CN)_6^{3-/4-}$ was used as a redox probe for monitoring changes on the modified electrode surfaces.

As shown in Fig. 1A, significant differences were observed in the electron transfer resistance with formation of the modified electrode surface. The impedance spectra includes two parts: a semicircle in the high frequency region (limited electron transfer) and a straight line in the low frequency region (limited diffusion process). The semicircle diameter indicates the electron transfer resistance; R_{ct}. Each electrochemical reaction is exhibited by an electric circuit. The most preferred model is the Randles–Ershler electric equivalent circuit model. It consists of the solution resistance (R_s), the charge-transfer resistance (R_{ct}), the Warburg resistance (Z_w) and the constant

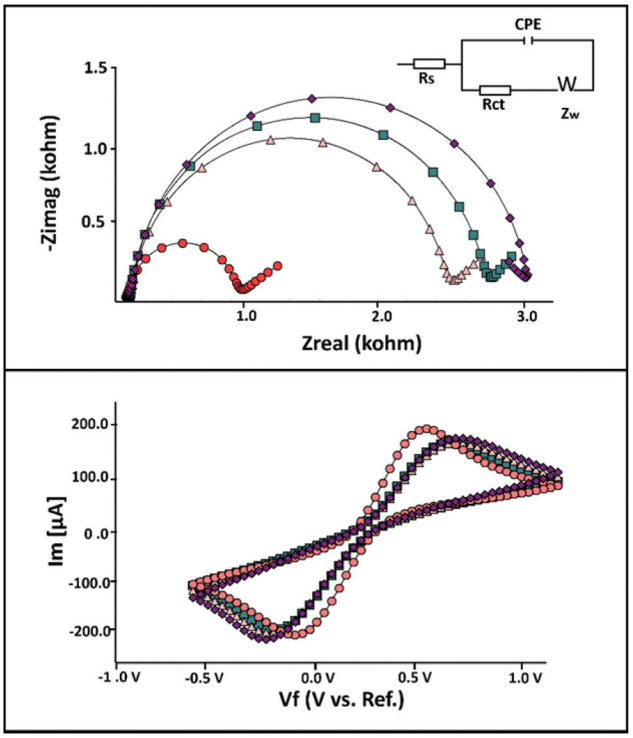

Fig. 1 The impedance spectra and cyclic voltammograms related to a modified ITO electrodes in a 0.1 M KCl solution containing 5.0 mM $K_3[Fe(CN)_6]/K_4[Fe(CN)_6]$. [The Nyquist impedance spectra (A) and cyclic voltammograms (B) obtained for the modification procedure are shown by different symbols:● ITO/OH, ◆ ITO/OH/TESU, ▲ ITO/OH/TESU/anti-RACK1 and ■ ITO/OH/TESU/anti-RACK1/BSA].

phase element (CPE). In our study, impedance values were fitted to Randles equivalent circuit simulation *via* Gamry Software (Reference 600, Gamry Instruments) and results corresponded to the Randles model. Nyquist diagrams showed that a difference in R_{ct} values between the aldehyde monolayers and hydroxylated ITO surface could be observed. The R_{ct} at the SAM modified electrode was higher than the hydroxylated ITO electrode because the formation of SAMs blocked the surface and it obstructed the electron transfer. The immobilization of anti-RACK1 antibodies onto the modified ITO surface with TESU was performed *via* covalent bonding between aldehyde groups on SAM and amino groups of the antibody. A decrease in the diameter of the semicircle of ITO/TESU/anti-RACK1 was observed after immobilization of the anti-RACK1 antibody. The remaining aldehyde sites were blocked by incubating in a BSA solution. As a result, the electrical resistance and the diameter of the semicircle were significantly increased. The increment in the value of R_{ct} after immobilization of BSA originated from the hindrance effect of proteins which are not conductive materials. EIS data presented that a successful fabrication of the immunosensor was achieved. The ITO based immunosensor had a rising impedimetric response to growing RACK1 antigen levels. These impedimetric responses illustrated the success of the immobilization steps and the immunosensor fabrication.

CV is an efficient tool to provide information about the alterations on the electrode surface after modification steps. This is because the alterations in the peak current are associated with electron transfer resistance. The reversible CV of the redox couple $[Fe(CN_6)]^{3-/4-}$ is exhibited in Fig. 1B. This redox couple exhibited typical voltammograms that have reversible oxidation and reduction peak currents on the ITO substrate. Also, the cyclic voltammetry results confirmed the impedance spectra results. For immobilization of the anti-RACK1 antibody to the ITO surface, a biocompatible surface was constructed using self-assembled monolayers onto the hydroxylated ITO electrodes. TESU is an excellent support material due to its reactive aldehyde groups on its end which bond amine groups covalently. The aldehyde groups on the ITO surface formed a densely packed monolayer, so peak current values decreased and the penetration of the redox couple also decreased. The aldehyde groups provided a covalent bonding point for biorecognition elements, which have amino groups on their surface. After the immobilization of the anti-RACK1 antibody, the peak values were decreased because of an insulating character of the protein for electron transfer. The small cathodic and anodic peaks were expected due to the insulating features of proteins, which inhibited the electron transfer to the electrode surface. In the BSA treatment, which was the last step for the fabrication of the immunosensor, BSA blocked free active ends (unbounded aldehyde ends bound free BSA) and also it prevented electron transfer between the electrolyte and electrode surface. BSA bonding on the electrode surface enhanced insulating properties of the electrode surface, which provided a more effective diffusion barrier, and decreased the peak current values. After binding the antigen, RACK1, the peak currents further decreased, also there was a deceleration in the electron transfer rate. In brief, after anti-RACK1 antibody immobilization and anti-RACK1 antibody-RACK1 antigen interactions, the anodic and cathodic peak currents decreased. The fall in the peak currents of the immunosensor originated from hindrance properties of the biorecognition event that reduced electron transfer between the electrolyte and electrode surface.

Morphological studies by using SEM

SEM characterization studies have been mostly performed for the evaluation of morphological features of modified electrodes. It provides excellent information related to chemical changes on any surface and covalent or physical immobilization process. The surface morphologies of the biosensor are shown in Fig. 2. The bare ITO electrode demonstrated a homogenous surface (Fig. 2A). The formed self-assembled monolayers are illustrated Fig. 2B. After immobilization of anti-RACK1, a uniform structure was observed on the ITO electrode (Fig. 2C). BSA had a globular morphology. Because of this, a globular form was seen on the ITO electrodes (Fig. 2D). The interaction between the anti-RACK1 antibody and RACK1 is illustrated in Fig. 2E. Results of SEM studies proved the accuracy of electrochemical impedance spectroscopy and cyclic voltammetry.

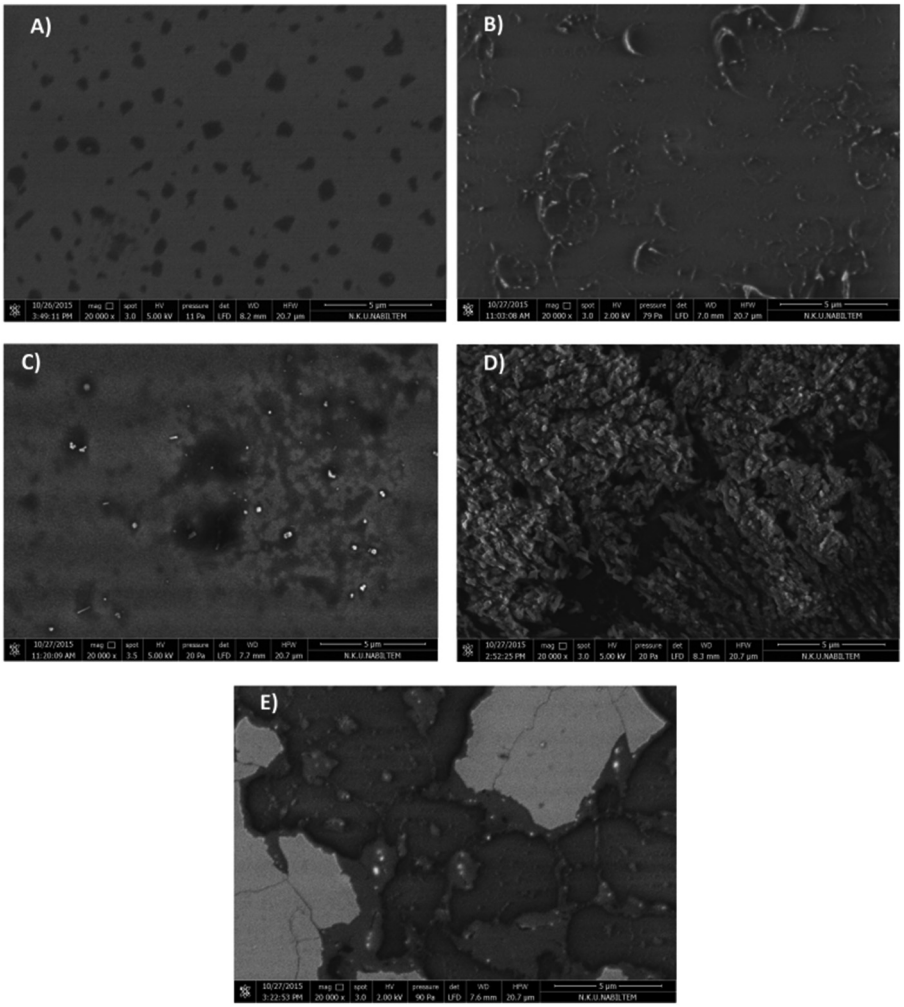

Fig. 2 SEM pictures taken for the different electrode surfaces obtained during biosensor fabrication [(A) ITO/OH; (B) ITO/OH/TESU; (C) ITO/OH/TESU/anti-RACK1; (D) ITO/OH/TESU/anti-RACK1/BSA; (E) ITO/OH/TESU/anti-RACK1/BSA/RACK1].

Optimization studies of the RACK1 biosensor

In order to develop a sensitive, repeatable and reproducible immunosensor, certain experimental factors such as TESU and antibody concentrations and antibody incubation time were optimized.

First of all, to evaluate the effect of concentration of TESU, the cleaned ITO substrate was incubated in different concentrations of TESU solution: 0.25%, 0.5%, 0.75% and 1%. An increment in the TESU concentrations caused a reduction in the charge transfer resistance and electrode signals. The signal of 0.25% and 0.75% TESU concentrations was similar and higher than that of the 0.5% TESU concentration. Therefore, 0.25% concentration was chosen as the optimum.

For investigating the effect of the anti-RACK1 antibody concentration on the formation of the biosensor sensing layer, different concentrations (0.325 ng mL^{-1}, 1.625 ng mL^{-1} and 4.85 ng mL^{-1}) were studied. Different anti-RACK1 concentrations affected the peak currents and the electron transfer resistances. For the low anti-RACK1 antibody concentration (0.325 ng mL^{-1}), as a sufficient amount of antibodies did not bind to the surface, a sensitive and valid response was not obtained. This result suggested that this antibody concentration was insufficient to capture the RACK1 antigen. As seen in the calibration curve for RACK1 (ESI Fig. 1†), the electron transfer resistance at this point did not reach the desired value. But, the calibration curve, which was obtained by using 1.625 ng mL^{-1} of the anti-RACK1 antibody, was linear. For the high concentration of the anti-RACK1 antibody, the linearity of the biosensor did not change. In accordance with the results, the optimum concentration of anti-RACK1 was chosen as 1.625 ng mL^{-1}.

The other optimization factor that should be optimized is the incubation period of the anti-RACK1 antibody. This also means the binding period of anti-RACK1 antibodies to SAMs. Because of this, TESU modified ITO electrodes were incubated into the anti-RACK1 antibody solutions for different durations such as 30 min, 45 min and 60 min. RACK1 calibration curves obtained for different anti-RACK1 incubation periods were shown in ESI Fig. 2.† The results illustrated that the

incubation period affected the binding of anti-RACK1 antibodies. For the 30 min incubation period, a sufficient amount of antibodies did not bind onto the modified electrode surface. 45 min and 60 min incubation periods were sufficient for covalent bonding of the anti-RACK1 antibody. R^2 values related to these incubation periods of 45 and 60 min were calculated as 0.9825 and 0.9839, respectively. The R^2 values were quite similar. Considering the calibration graphs and R^2 values, 45 min was chosen as the optimum incubation period, which was enough for the immobilization of the anti-RACK1 antibody.

Finally, the incubation period of the RACK1 antigen was optimized. This optimization parameter is also important because it affects the antibody–antigen binding process directly. For this purpose, four different incubation periods were tested. The result obtained in 30 and 45 min pointed that these incubation periods of RACK1 were not enough to bind to anti-RACK1. Other incubation periods (60 and 75 min) were enough to bind anti-RACK1. In this circumstance, the R^2 and calibration values were investigated and 60 min was chosen as the optimum incubation duration for RACK1.

Analytical characteristics of the biosensor

The analytical performance of the proposed immunosensor was explored by quantifying the standard RACK1 solution with different concentrations under optimized conditions. A linear relevance was found between RACK1 concentrations and the change in the charge transfer resistances, which were calculated by using the equivalent circuit model inserted in Fig. 1A. This equivalent circuit model contains an ohmic resistance (R_s) related to the resistance of the electrolyte solution, charge transfer resistance (R_{ct}), double layer capacitance regarding with the capacitance of the complex bioactive layer, and the Warburg impedance (Z_w) reflecting the normal diffusion to the electrode surface through the complex layer.

In the light of this information, the calibration curve of the RACK1 immunosensor was drawn by means of impedimetric responses, which was calculated as given:

$$\Delta R_{ct} = R_{ct}(\text{RACK1}) - R_{ct}(\text{BSA})$$

R_{ct}(RACK1) is the value of the semicircle diameter (charge transfer resistance) after the RACK1 antigen bound to the biosensor (it corresponds to antibody–antigen interactions). R_{ct}(BSA) is the value of the semicircle diameter of the immunosensor layer after fabrication. Sensitivity analysis for the RACK1 antigen was evaluated by means of the ΔR_{ct} results.

Fig. 3 presents the voltammograms and Nyquist plots of the immunosensor incubated in increasing concentrations of the RACK1 antigen. The variations of these semicircle diameters shown in Nyquist plots were evaluated as a response to determine the interaction between anti-RACK1 and RACK1. The semicircle diameter of the Nyquist plot (Fig. 3A) increased with increasing RACK1 concentration. The range of biosensor sensitivity was found between 14.25 fg mL^{-1} and 712.5 fg mL^{-1} with a coefficient of 0.99% (Fig. 3B) and limit of detection (LOD; 3 fold of standard deviation) and limit of quantification

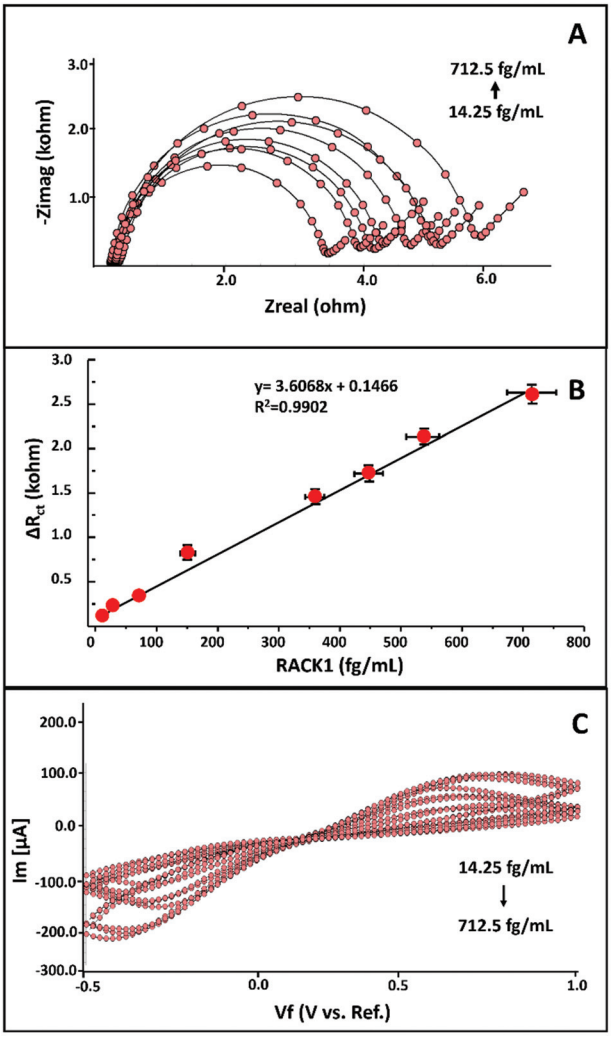

Fig. 3 RACK1 calibration curve study for the biosensor based on ITO modified TESU. (A) Impedance spectra obtained for the different RACK1 concentrations in a 0.1 M KCl solution containing 5.0 mM $K_3[Fe(CN)_6]/K_4[Fe(CN)_6]$ (inserted Fig. 1A shows the electrical equivalent circuit model used for the impedance calculations). (B) RACK1 linear calibration plot drawn by the impedance differences extracted from (A). (C) CVs obtained for the different RACK1 concentrations in a 0.1 M KCl solution containing 5.0 mM $K_3[Fe(CN)_6]/K_4[Fe(CN)_6]$.

(LOQ; 10 fold of standard deviation) of 30 fg mL^{-1} and 100 fg mL^{-1}, respectively. These results indicate that the interactions between the anti-RACK1 antibody and RACK1 antigen can be sensed by this developed electrode. Fig. 3C illustrates the CVs of the immunosensor with the increasing concentrations of the RACK1 antigen. After the biorecognition event between anti-RACK1 and the RACK1 antigen, the CV peaks of the redox couple decreased. The peak current values were inversely proportionate to the concentration. The reason for this circumstance is the increasing amount of RACK1 on the electrode surface. So this increase caused a decrease in the electron transfer between the electrolyte and electrode surface because of the insulating character of the proteins. In brief, a gradual increment in the RACK1 concentration caused a

gradual decrease in both anodic and cathodic peak currents and a gradual increase in the impedance value.

EIS and CV methods were assessed for monitoring of immobilization and characterization of the presented immunosensor. Another technique, square wave voltammetry (SWV) was also applied to prove CV and EIS results. The SWV peaks were investigated and it was found that the peak currents decreased after binding of RACK1 antigens onto each electrode. Moreover, the differences between BSA peak currents and RACK1 peak currents increased because of the interaction with more RACK1 antigen molecules bound to the electrode surface. Also, the peak currents and RACK1 concentrations had a linear relationship. The calibration curve is displayed in Fig. 4.

Although the SWV technique was used in the RACK1 analyses, the sensitivity obtained by this electrochemical method was slightly less than the other methods of EIS and CV. The results demonstrated that the linear calibration range of the biosensor for RACK1 was obtained between 28.5 fg mL^{-1} and 535 fg mL^{-1}, which was narrower than the linear calibration range obtained by the EIS method (14.25 pg mL^{-1} and 712.5 pg mL^{-1}), as shown in Fig. 4.

The repeatability of the immunosensor was investigated for three different RACK1 concentrations (low, medium, high) by using equally prepared biosensors. By these repeatability experiments, the correlation coefficient, average value and standard deviation for the low (28.5 fg mL^{-1}), medium (142.5 fg mL^{-1}) and high (712.50 fg mL^{-1}) RACK1 concentrations in the linear range were calculated as 7.2%, 28.84 fg mL^{-1} and 2.07 fg mL^{-1}; 7.32%, 140.2 fg mL^{-1} and 10 fg mL^{-1}; 3.19%, 720.89 fg mL^{-1} and 23.03 fg mL^{-1}, respectively.

The reproducibility of the RACK1 immunosensor was tested using different biosensors fabricated by the same procedures (10 RACK1 calibration plots were drawn by using at least 80 disposable biosensors). These immunosensors were fabricated independently under the same conditions. All of these immunosensors showed the same linearity in the range between 14.25 fg mL^{-1} and 712.5 fg mL^{-1} for RACK1. The relative standard deviations were also calculated by using the slopes and the intercepts of the linear equations obtained from these biosensors as 5.15% and 6.11%, respectively. These results clearly indicated that the new biosensor shows excellent reproducibility and good repeatability and sensitivity for RACK1 determination. Our results indicated the applicability of TESU monolayers as an excellent material for immobilizing biorecognition elements for the fabrication of a new immunosensor for the RACK1 antigen.

The lifetime of the ITO based disposable biosensor was also evaluated by monitoring the electrochemical signals at the end of the various periods. During the storage period, ITO biosensors were stored at 4 °C. Our biosensor presented good performance during the first 8 weeks. There was a slight decrease in the activity at the end of the 8th week. The ITO based immunosensor modified with TESU retained 88.24% of its initial activity after an 8 week storage period. However, on the 9th week the immunosensor did not give a response (Fig. 5). Also at the end of this period, the surface of the electrode got damaged. The result demonstrated that the biosensor could be used over a long period when it was stored at 4 °C.

Reusability is a key factor in the application and development of immunosensors. Despite the antibody–antigen linkage that can be broken under drastic conditions (alkaline or acidic conditions), functional properties of the immobilized biorecognition elements still continue for a while. For testing of reusability of the immunosensor, it was exposed to an acidic solution (ultra-pure water: HCl, 0.1%) for 5 min. The immunosensor was regenerated for three cycles and after 3 cycles the electrode surface became damaged and also it lost its immunoreaction capacity. Although the presented immunosensor had a disposable design, reusability was demonstrated in terms of regeneration capability. After the first regeneration step, the immunosensor saved 88% of its initial activity. At the end of the second regeneration, it retained 81% of its initial activity. At the end of the third regeneration step, the ITO based electrode was damaged. These studies illustrated the relative robustness of the ITO based immunosensors.

Real or artificial sample analyses are important for the investigation of the performance of an immunosensor. First of all, sample analysis performance of the presented immuno-

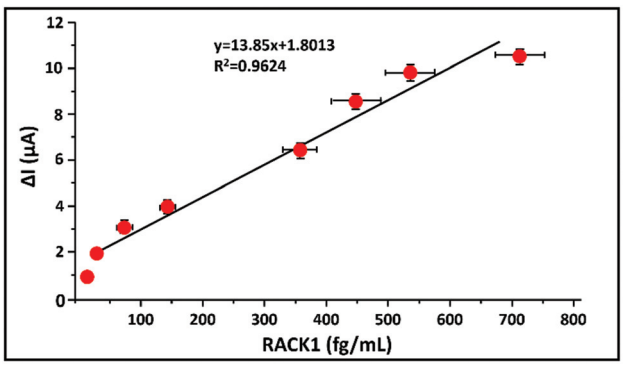

Fig. 4 RACK1 calibration curve obtained by the SWV in a 0.1 M KCl solution containing 5.0 mM $K_3[Fe(CN)_6]/K_4[Fe(CN)_6]$.

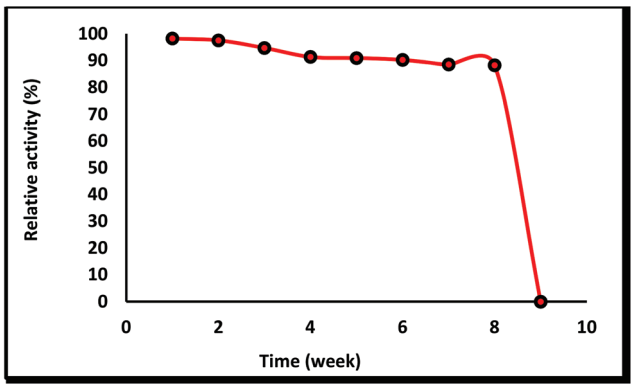

Fig. 5 The storage stability of the developed immunosensor.

Table 1 RACK-1 determination in human serum samples

Sample	Found by biosensor (fg mL^{-1})	Added RACK1 (fg mL^{-1})	Total found by biosensor	% Recovery	% Relative difference
1	158.9	142.5	297.7	98.8	−1.2
2	349.1	142.5	479.2	97.5	−2.5
3	271.2	142.5	400.2	96.7	−3.3
4	134.1	142.5	264.3	95.6	−4.4
5	243.6	142.5	371.1	96.1	−3.9

sensor was examined by using artificial serum samples. The artificial serum samples spiked with RACK1 antigen were measured with the newly developed immunosensor (the results are given in the ESI†).

Secondly, to examine the practical applicability of the proposed immunosensor, a series of human serum samples obtained from Namık Kemal University Hospital were analysed (with the ethics committee approval). Serum samples were firstly tested directly by the proposed biosensor. Then we used the standard addition method by adding 142.5 fg mL^{-1} of RACK1 to the real human serum samples (all tests were done in duplicate). The obtained results are shown in Table 1. From Table 1, it can be seen that the recovery and relative standard deviation values range from 94.6% to 101.3% and −6.3% to 1.3%, respectively. These results indicated that the developed immunosensor can be used in real biological samples.

Conclusion

In this work, we successfully fabricated disposable, ITO based flexible working electrodes for sensing the interaction between RACK1 antigen and anti-RACK1 antibody. Anti-RACK1 antibody was first utilized as a biorecognition element in this study. It was proven that TESU provided an excellent new immobilization agent for the effective and practical immobilization of different kinds of proteins onto ITO substrates. Moreover the investigations showed that TESU based biosensors enabled the production of reproducible and high sensitive analysis of RACK1. Optimization parameters which may affect the sensitivity of ITO electrodes, such as antibody concentration and antibody incubation time were also investigated. A low LOD (30 fg mL^{-1}) and LOQ (100 fg mL^{-1}) and a wide detection range (14.25–712.5 fg mL^{-1}) were obtained by using the simple, rapid electrochemical immunosensor based on disposable ITO electrodes. SEM and SWV studies proved the result's accuracy. The lifetime of the immunosensor was relatively long, which is an important parameter for clinical applications. Our immunosensor could be regenerated and so it could be used for more than one measurement. Moreover, our biosensor was successful in the analysis of artificial serum samples spiked with RACK1 and real human serum samples. Briefly, the developed immunosensor showed acceptable performance for the detection of the RACK1 antigen, exhibited a low detection limit, and had selective and reproducible results in the immunoreaction. Finally, it is suggested that TESU should effectively be used in other biosensor fabrication processes because of its excellent fitting with ITO based substrates.

Acknowledgements

The authors acknowledge financial support from The Scientific and Technological Research Council of Turkey (TÜBİTAK) (Project Number: 113 Z 678).

References

1 D. R. Adams, D. Ron and P. A. Kiely, *Cell Commun. Signaling*, 2011, **9**(22), 1–24.
2 R. Nagashio, Y. Sato, T. Matsumoto, T. Kageyama, Y. Satoh, R. Shinichiro, N. Masuda, N. Goshima, S. Jiang and I. Okayasu, *Lung Cancer*, 2010, **69**, 54–59.
3 Q. Ren, J. Zhou, X. Zhao and J. Wang, *Dev. Comp. Immunol.*, 2011, **35**, 629–634.
4 S. Kraus, D. Gioeli, T. Vomastek, V. Gordon and M. J. Weber, *Cancer Res.*, 2006, **66**(22), 1–9.
5 X. Cao, J. Xu, X. Liu, J. Xu, W. Wang, Q. Li, Q. Chen, Z. Xu and X. Liu, *Int. J. Cancer*, 2010a, **127**, 1172–1179.
6 Z. Wang, B. Zhang, L. Jiang, X. Zeng, Y. Chen, X. Feng, Y. Guo and Q. Chen, *Eur. J. Cancer*, 2009, **45**, 490–496.
7 X. Cao, X. Xu, J. Xu, X. Liu, Y. Cheng, W. Wang, Q. Li, Q. Chen, Z. Xu and X. Liu, *Breast Cancer Res. Treat.*, 2010b, **123**, 375–386.
8 J. Lacombe, A. Mange, M. Jarlier, C. Bascoul-Mollevi, P. Rouanet, P. Lamy, T. Maudelonde and J. Solassol, *Int. J. Cancer*, 2013, **132**, 1105–1113.
9 M. Özmen, K. Can and M. Ersoz, *J. Electroanal. Chem.*, 2009, **633**, 228–234.
10 M. Barreiros dos Santos, S. Azevedo, J. P. Agusi, B. Prieto-Simón, C. Sporer, E. Torrents, A. Juárez, V. Teixeira and J. Samitier, *Bioelectrochemistry*, 2015, **101**, 146–152.
11 L. Yang and Y. Li, *Biosens. Bioelectron.*, 2005, **20**, 1407–1416.
12 H. Zeng, D. A. Y. Agyapong, C. Li, R. Zhao, H. Yang, C. Wu, Y. Jiang and Y. Liu, *Sens. Actuators, B*, 2015, **221**, 22–27.
13 M. Ç. Canbaz and M. K. Sezgintürk, *Anal. Biochem.*, 2014, **446**, 9–18.
14 M. N. Sonuç and M. K. Sezgintürk, *Curr. Anal. Chem.*, 2016, **12**(1), 43–53.
15 M. N. S. Karaboğa, Ç. S. Şimşek and M. K. Sezgintürk, *Biosens. Bioelectron.*, 2016, **84**, 22–29.
16 G. Kim, K. Kim, M. Oh and Y. Sung, *Biosens. Bioelectron.*, 2010, **25**, 1717–1722.
17 V. Dharuman, J. H. Hahn, K. Jayakumar and W. Teng, *Electrochim. Acta*, 2013, **114**, 590–597.
18 A. K. Yagati, T. Lee, J. Min and J. Choi, *Colloids Surf., B*, 2012, **92**, 161–167.
19 Y. Wang, W. Qian, Y. Tan, S. Ding and H. Zhang, *Talanta*, 2007, **72**, 1134–1140.
20 J. Lin, L. Zhang and S. Zhang, *Anal. Biochem.*, 2007, **370**, 180–185.

21 J. Wang, L. Wang, J. Di and Y. Tu, *Sens. Actuators, B*, 2008, **135**, 283–288.
22 A. I. Gopalan, K. Lee and D. Ragupathy, *Biosens. Bioelectron.*, 2009, **24**, 2211–2217.
23 E. Zor, I. H. Patir, H. Bingol and M. Ersöz, *Biosens. Bioelectron.*, 2013, **42**, 321–325.
24 J. Zhang, M. C. Pearce, B. P. Ting and J. Y. Ying, *Biosens. Bioelectron.*, 2011, **27**, 53–57.
25 S. K. Arya, A. K. Prusty, S. P. Singh, P. R. Solanki, M. K. Pandey, M. Datta and B. D. Malhotra, *Anal. Biochem.*, 2007, **363**, 210–218.
26 Y. Song, Y. Ma, Y. Wang, J. Di and Y. Tu, *Electrochim. Acta*, 2010, **55**, 4909–4914.
27 M. Lee, N. Zine, A. Baraket, M. Zabala, F. Campabadal, R. Caruso, M. G. Trivella, N. Jaffrezic-Renault and A. Errachid, *Sens. Actuators, B*, 2012, **175**, 201–207.
28 B. Ibarlucea, C. Fernandez-Sanchez, S. Demming, S. Büttgenbach and A. Llobera, *Analyst*, 2011, **136**, 3496–3502.
29 M. Lee, A. Baraket, N. Zine, M. Zabala, F. Campabadal, N. Jaffrezıc-Renault and A. Errachıd, *Sens. Transducers J.*, 2014, **27**, 233–238.